

Fracture Toughness of Polymer Interface Reinforced With Diblock Copolymer: Effect of Homopolymer Molecular Weight

Chi-An Dai[†] and Edward J. Kramer*

Department of Materials Science and Engineering and the Materials Science Center,
Cornell University, Ithaca, New York 14853

Junichiro Washiyama

Kawasaki Development Center, Japan Polyolefins Company, Ltd., 3–2, Chidori-Cho,
Kawasaki-Ku, Kawasaki, Kanagawa, 210, Japan

Chung-Yuen Hui

Department of Theoretical and Applied Mechanics and the Materials Science Center,
Cornell University, Ithaca, New York 14853

Received April 9, 1996; Revised Manuscript Received August 13, 1996[®]

ABSTRACT: We have measured the fracture toughness, G_c , of an immiscible polymer/polymer [polystyrene (PS) and poly(2-vinylpyridine) (PVP)] interface reinforced with deuterium-labeled dPS-*b*-PVP diblock copolymers as a function of the number-average molecular weight, \bar{M}_n , of the polystyrene homopolymer, either monodisperse homopolymer PS (MPS) or polydisperse homopolymer PS (PPS). The dependence of G_c on the PS molecular weight was investigated at different areal chain densities, Σ , of the copolymers. These values of Σ were chosen to be in either one of two fracture mechanism regimes: chain scission or crazing. In the chain scission regime, G_c is independent of the molecular weight of MPS and PPS. In contrast in the crazing regime (for $\Sigma \leq \Sigma_{\text{sat}}$, where Σ_{sat} is the saturation Σ for the copolymer at the interface), \bar{M}_n of MPS has a strong effect on the fracture toughness. For this case, G_c increases sharply around $\bar{M}_n \approx 100\,000$ and then levels off at higher \bar{M}_n values. The polydisperse PS/PVP interface has a fracture toughness consistent with its \bar{M}_n rather than its weight-average molecular weight, \bar{M}_w . When the interface is covered with copolymer lamellae ($\Sigma \gg \Sigma_{\text{sat}}$), G_c is found to be independent of \bar{M}_n of the MPS and is substantially larger than that for the PPS/PVP interface at the same Σ . For the PPS/PVP interface, the low molecular weight portion of PPS swells the lamellar structure, resulting in a decrease in G_c compared to that of the MPS/PVP interface. We have also measured G_c as a function of composition of a blend of high and low \bar{M}_n MPS, where \bar{M}_n of the low molecular weight PS is below the entanglement molecular weight of PS. Dilution of the entanglement density of the homopolymer polystyrene results in a strong decrease in G_c . Our results are compared with recent models for craze failure. A continuum craze model using the full stress field proposed by Sha et al.²⁰ predicts the fracture toughness better than models^{2,9} using the asymptotic stress field.

Introduction

Polymer interfacial adhesion is of interest because of its importance in polymer blends, lamination of polymer composites, and polymer processing. However, interfaces between immiscible homopolymers are normally weak, as there are few chains which can penetrate far enough into the opposite homopolymer to become entangled there. It is well-known that the addition of A–B diblock copolymers to immiscible glassy homopolymers improves the mechanical properties, particularly the fracture toughness of the polymer interfaces.^{1–3} Block copolymers form interphase “connectors” through which the stress can be transferred across the interface. Recent studies^{4–8} show that the effectiveness of the reinforcement depends primarily on the areal chain density (number of chains per unit area), Σ , of the block copolymer at the interface, the molecular weight of each block (M_A and M_B), and the entanglement molecular weight (M_e) of the two homopolymers. Several microscopic mechanisms of interfacial failure are identified and summarized below.

(1) Chain scission of the A–B diblock copolymer, where the chain breaks near the joint in the block copolymer, before any large scale plastic deformation of the homopolymers occurs, can occur when Σ of the block copolymer is small and $M_A, M_B \gg M_e$.

(2) Chain pull-out, where one of the blocks of the copolymer chain pulls out from the surrounding homopolymer, generally occurs if either M_A or $M_B < M_e$.

(3) Large scale plastic deformation, where crazing (a cavitation mode of plastic deformation resulting in a fine fibrillar polymer/void microstructure) of the homopolymer takes place near the interface followed by craze fibril failure, occurs by either chain disentanglement or chain scission or a mixture of these two mechanisms in the craze fibrils.

The most important interface failure mechanism is crazing since the fracture toughness, G_c of the interface can be greatly enhanced if crazing occurs. The fracture toughness G_c is the energy required per unit area of crack tip advance. In glassy polymers G_c is usually much larger than twice the surface energy because of the much larger energy dissipated by a zone of plastic deformation ahead of the crack tip. In most glassy polymers, the most important form of this crack tip plasticity is crazing and thus fracture of these polymers is found to be governed by the growth and breakdown of crazes ahead of the crack tip. Once craze fibril breakdown occurs, voids can form in the craze and

* To whom correspondence should be addressed.

[†] Current address: Manufacturing Research & Engineering Organization, Materials Science and Engineering Division, Eastman Kodak Company, Rochester, NY 14652-3701.

[®] Abstract published in *Advance ACS Abstracts*, October 15, 1996.

subsequently grow into cracks leading to the fracture of the entire specimen.

Currently, the best model for craze failure ahead of a crack tip is that originally proposed by Brown.² An important consideration in Brown's theory is that the cross-tie fibrils (fibrils that connect main fibrils) can transfer stress between the main fibrils. This load transferring mechanism allows the stress of the fibril at the crack tip to reach the breaking stress of the polymer chains. By assuming that all the craze fibrils fail by chain scission, Brown derived a formula that relates the fracture toughness to the anisotropic elastic properties of the craze and the entanglement density of the crazed material.

In an attempt to generalize Brown's model to the chain disentanglement case, de Gennes¹¹ proposed that a craze fails in the "active zone" at the craze-bulk interface where polymer chains are drawn into fibrils. His model predicts that G_c should scale as M^2 , where M is the molecular weight of the polymer chains.

To predict G_c of a polymer interface reinforced with block copolymers, a detailed understanding of the areal density of entangled strands bridging between the diblock copolymers and the homopolymer is needed. Logically this areal density of strands should be dependent on homopolymer molecular weight since homopolymer chain ends cannot participate in the entanglement network. However, although most diblock copolymers were nearly monodisperse, the homopolymers used in previous experiments were usually of commercial grade and polydisperse. Even so, no experiments examining the effects of molecular weight of the polydisperse homopolymers have been carried out.

In this paper, we investigate the fracture toughness of the interfaces between immiscible homopolymers reinforced with diblock copolymers as a function of molecular weight of the homopolymer. Part of the objective of this work was to explore the difference in the fracture toughness between polydisperse and monodisperse homopolymers. The experiments are carried out with different areal chain densities of copolymers at the interface which result in the interfaces failing by different failure mechanisms. At small Σ , the chain scission mechanism is active. At larger Σ , for both $\Sigma \leq \Sigma_{\text{sat}}$ and $\Sigma \geq \Sigma_{\text{sat}}$, crazing fracture dominates, where Σ_{sat} is the saturation areal density of the copolymer at the interface below which the copolymers organize themselves as a polymer brush and above which copolymers form additional layers of lamellae at the interface. A test of the importance of entanglements for the fracture toughness is also carried out using a bimodal molecular weight blend as the homopolymer. This blend is formulated by diluting high molecular weight polymer with chains that are too short to entangle.

The system we have chosen consists of the immiscible homopolymers polystyrene (PS) and poly(2-vinylpyridine) (PVP). PS and PVP have approximately the same glass transition temperature ($T_g \sim 105^\circ\text{C}$). Thus, there is almost no residual stress upon cooling bilayer samples from the molten state. Both homopolymers deform predominately by crazing; however, PS has a smaller crazing stress than PVP (≈ 55 MPa for PS and ≈ 75 MPa for PVP). The formation of a wide craze ahead of the crack tip can be easily recognized by inspecting the fracture surfaces with an optical microscope. Moreover, the Flory interaction parameter of the PS/PVP system is large and positive ($\chi \approx 0.12$ at 160°C)¹² leading to

Table 1. Characterization of Homopolymers and Block Copolymers

homopolymers			block copolymers		
code	\bar{M}_n	\bar{M}_w/\bar{M}_n	code	N_{PS}	N_{PVP}
PS	130 000	~ 2.1	800–870	800	870
PVP	110 000	~ 2.4	510–540	510	540

strong immiscibility and weak PS/PVP interfaces in the absence of diblock copolymer.

Experimental Section

1. Materials: Polydisperse PS (PPS) and monodisperse PS (MPS) homopolymers are both used in this study. Polydisperse PS and PVP homopolymers purchased from Aldrich Chemical Co. and Polysciences Co., respectively, were of commercial grade with number-average molecular weights (\bar{M}_n) of 130 000 and 110 000, respectively. Several different samples of nearly monodisperse PS were purchased from Pressure Chemical Co. and had \bar{M}_n ranging from 70 000 to 1 800 000. The polydispersity indices of these MPS are 1.15 or less. The characteristics of the dPS-*b*-PVP diblock copolymers used in this study are shown in Table 1. The diblock copolymer consisting of a PS block with a degree of polymerization of 800 and PVP block of 870 will be designated as 800–870. The number-average molecular weight for each block of each copolymer chain is larger than M_e ($M_{e\text{PS}} \approx 18$ 000, $M_{e\text{PVP}} \approx 27$ 000). The polystyrene blocks of the copolymers were deuterated in order to allow for their use as labels in the subsequent FRES experiments. The FRES technique utilizes a ^4He ion beam impinging on an area ~ 5 mm \times 1 mm of each fracture surface of the sample.¹³ The energy of recoiled hydrogen and deuterium particles is recorded and converted into a depth scale based on the energy loss of the particles on their path through the sample. The amount of deuterium averaged over the probe area on each fracture surface is determined by integrating its spectrum signal in FRES which is readily converted into an apparent areal chain density, Σ , of the deuterated PS block of the copolymer on each side of the fracture [$\Sigma(\text{PS})$ and $\Sigma(\text{PVP})$]. The total areal chain density is then given by

$$\Sigma = \Sigma(\text{PS}) + \Sigma(\text{PVP})$$

2. Sample Preparation. Plates of polydisperse PS and PVP with dimensions of 5 cm \times 7 cm \times 2.4 mm and 5 cm \times 7 cm \times 1.7 mm, respectively, were made by compression molding at 160°C . A thin film of the block copolymer was spun cast from a toluene solution onto the PVP plate. The thickness of the copolymer film or the areal chain density, Σ , of the copolymer is controlled by the concentration of the copolymer solution that is spun onto the PVP plate. Since it is impractically expensive to use monodisperse PS sample plates for the fracture toughness measurement, we developed a "glazing method". The method is as follows: a film of monodisperse polystyrene (MPS) (~ 60 μm thick) is made by casting a monodisperse PS solution onto a glass plate mold. After drying for 12 h to remove any excess solvent, the MPS film was floated off the glass plate onto the surface of a water bath and picked up on the block-copolymer-coated PVP plate. The MPS/copolymer/PVP assembly was then annealed at 160°C for 2 h. The backing PPS plate was then joined with the annealed MPS/copolymer/PVP plates at 140°C for only 20 min. This welding time was chosen to be long enough so that good adhesion was obtained between the polydisperse PS and the monodisperse PS but to be short enough that the low molecular weight portion of the polydisperse PS can not diffuse through the monodisperse PS film to reach the block copolymer brush, thereby affecting the entanglement between the block copolymer and the MPS. The final PPS/MPS/copolymer/PVP sandwich plate was then cut into eight strips for the fracture measurements. A schematic of the sample geometry is shown in Figure 1. Monodisperse PVP homopolymer is not needed or used in our study since we believe that the molecular weight for both the PVP homopolymer and the block copolymer is high enough such that PVP block of the copolymer is well-anchored

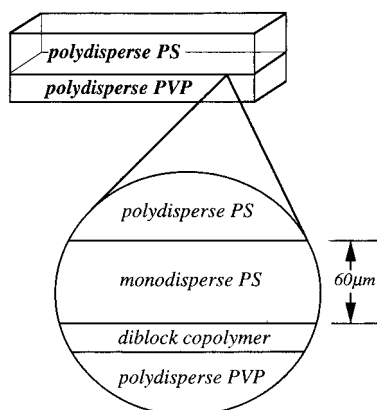


Figure 1. A schematic drawing of PS/PVP test sample showing details of the sandwich structure.

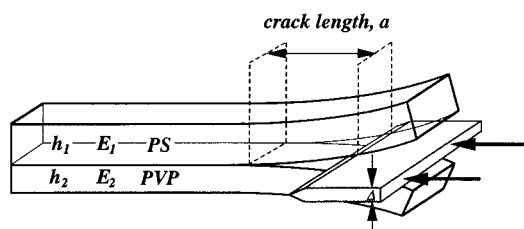


Figure 2. Schematic of the ADCB method used for the fracture toughness test.

on the PVP homopolymer side of the interface even at relatively high fracture toughnesses, where crazing occurs on the PS side of the interface. Crazing, and therefore the breakdown of the craze at the crack tip, is not observed on the PVP side of the interface. The deuterium distribution on the two sides of the fracture, as well as previous studies¹⁴ of the plastic deformation ahead of the crack tip by transmission electron microscopy, supports this claim.

3. Fracture Toughness Measurement. The interfacial fracture toughness, or the critical energy release rate, G_c , is measured using the asymmetric double cantilever beam method (ADCB). A schematic drawing of this method is shown in Figure 2. A razor blade of known thickness, Δ , is inserted into the PS/PVP interface. A crack is initiated ahead of the razor blade. This razor blade is then driven by a servo motor at a constant speed (3×10^{-6} m/s) into the interface. Steady state crack propagation was established after several minutes. The entire history of crack progression, in particular the length, a , of the crack ahead of the razor blade, was recorded using a video camera so that many measurements of a could be made using one PS/copolymer/PVP strip. The error bars reported subsequently for G_c represent one standard deviation of at least 16 crack length measurements. The crack length a is converted to G_c using the relation first developed by Kanninen¹⁵ and later modified by Creton *et al.*³, i.e.

$$G_c = \frac{3\Delta^2}{8\alpha^4} (E_1 E_2 h_1^3 h_2^3) \frac{(C_1^2 E_2 h_2^3 + C_2^2 E_1 h_1^3)}{(C_1^3 E_2 h_2^3 + C_2^3 E_1 h_1^3)^2}$$

where $C_1 = 1 + 0.64h_1/a$ and $C_2 = 1 + 0.64h_2/a$. E_1 and E_2 are the Young's moduli and h_1 and h_2 are the thickness of PS and PVP homopolymer beams, respectively.

It should be noted that as a crack propagates along an interface between two materials with different elastic moduli, the stress field of the crack tip along the interface in general has both tensile (mode I) and shear (mode II) components. A phase angle, Ψ , is defined as a measure of the relative shear to the opening components. To assure that the crack propagates at the PS/PVP interface, the plate of the more compliant material (PS) was made to be thicker than the PVP plate, giving rise to a mechanical phase angle $\Psi \approx -6^\circ$. At this value of Ψ , the fracture toughness of the interface is a minimum and is only weakly dependent on Ψ as long as $\Psi < 0$. A

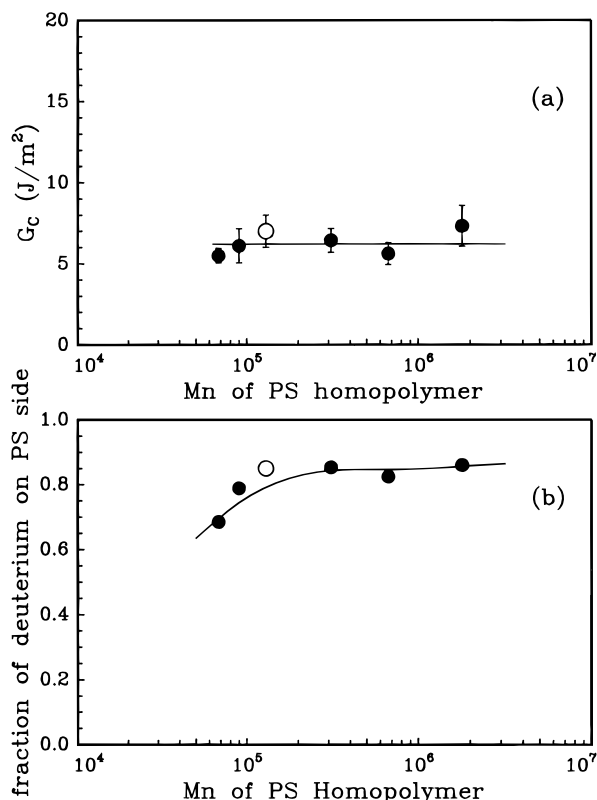


Figure 3. (a) The fracture toughness of the interface is plotted as a function of number average molecular weight of (●) the monodisperse homopolymer PS and (○) the polydisperse PS at $\Sigma = 0.025$ chains/nm² of the 800–870 diblock copolymer. (b) Fraction of the deuterium found on the PS fracture surface, P , plotted versus molecular weight of MPS.

detailed discussion of the effects of Ψ on fracture of PS/PVP interfaces reinforced with diblock copolymers can be found in the work of Xiao *et al.*¹⁶

Results

1. Chain Scission at Small Areal Chain Density.

Figure 3a shows the fracture toughness, G_c , of the PS/PVP interface as a function of the number-average molecular weight, \bar{M}_n , of the monodisperse homopolymer PS (MPS) at an areal chain density (Σ) ≈ 0.025 chains/nm² of 800–870 diblock copolymer. The plot also includes G_c data for the interface between polydisperse PS (PPS) and PVP for the same Σ of the 800–870 diblock copolymer. The G_c values for both PPS and MPS are low (~ 5 – 7 J/m²). In addition, the G_c values are nearly independent of the \bar{M}_n of the MPS. Optical microscopy of the fracture surface shows that there is no significant plastic deformation in the form of crazing. In Figure 3b, the fraction of deuterium found on the PS side of the fracture surface, P , is plotted as a function of Σ . For $\bar{M}_n \geq 100\,000$, most but not all the deuterium (~ 80 – 90%) is found on the PS side of the interface. For $\bar{M}_n \leq 100\,000$, the fraction of deuterium on the MPS side of the fracture decreases slightly to ~ 60 – 70% .

The above result for the MPS is consistent with that for the PPS/PVP interface studied previously by Creton *et al.*³ Below a critical Σ ($\Sigma^* = 0.03$ chain/nm²), the interface fails by chain scission of the block copolymers near their joints without any significant plastic deformation. The G_c values are low since there are too few diblock copolymers per unit area bridging the interface. The block copolymer chains break before the interfacial stress can increase enough to cause plastic deformation. The deuterium distribution plot (P vs \bar{M}_n) plot in Figure

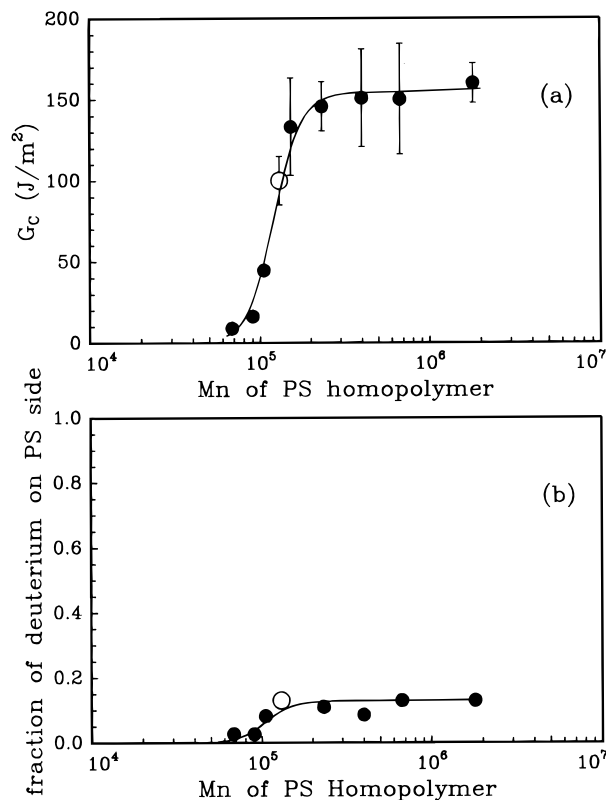


Figure 4. (a) The fracture toughness of the interface is plotted as a function of number average molecular weight of (●) the monodisperse homopolymer PS and (○) the polydisperse PS at $\Sigma = 0.09$ chains/nm² of the 800–870 diblock copolymer. (b) Fraction of the deuterium found on the PS fracture surface, P , plotted versus molecular weight of MPS.

3b) shows that the block copolymer chains break near the joint for $\bar{M}_n \geq 100\,000$. For $\bar{M}_n \leq 100\,000$, some of the copolymers seem to be disentangled from the homopolymer matrix, resulting in the decrease in the fraction of deuterium on the MPS side of the fracture.

2. Craze Fracture at Medium Areal Chain Density ($\Sigma \leq \Sigma_{\text{sat}}$). In Figures 4a and 5a, the fracture toughness of the PS/PVP interface is plotted as a function of \bar{M}_n of the homopolymer PS for $\Sigma \approx 0.09$ chains/nm² of the 800–870 diblock copolymer and for $\Sigma \approx 0.10$ chains/nm² of the 510–540 diblock copolymer, respectively. The plots of G_c vs \bar{M}_n for both copolymers show very similar features. There is a regime in both plots where G_c remains roughly constant: at high \bar{M}_n ($\bar{M}_n \geq 150\,000$), the fracture toughness has a plateau value of ~ 150 J/m² for the 800–870 diblock copolymer and ~ 60 J/m² for the 510–540 diblock copolymer. G_c decreases by 1–2 orders of magnitude for both diblock copolymers as \bar{M}_n decreases from $\sim 150\,000$ to $\sim 70\,000$. The interface between polydisperse PS ($\bar{M}_n \approx 130\,000$) and PVP, indicated by an open circle in the figures, has a fracture toughness of about 100 and 35 J/m² for the 800–870 and 510–540 diblock copolymers, respectively. The polydisperse PS/PVP interface has a fracture toughness consistent with its \bar{M}_n for both copolymers. In contrast, if G_c were assumed to correlate with the weight-average molecular weight \bar{M}_w , the agreement between G_c for the polydisperse PS/PVP interface and the monodisperse PS/PVP interface would be very poor. Clearly number-average molecular weight is the moment of the molecular weight distribution that controls the interface fracture toughness in this regime. In Figures 4b and 5b, the fraction of the deuterium on the PS side of the fracture is plotted as a function of \bar{M}_n of

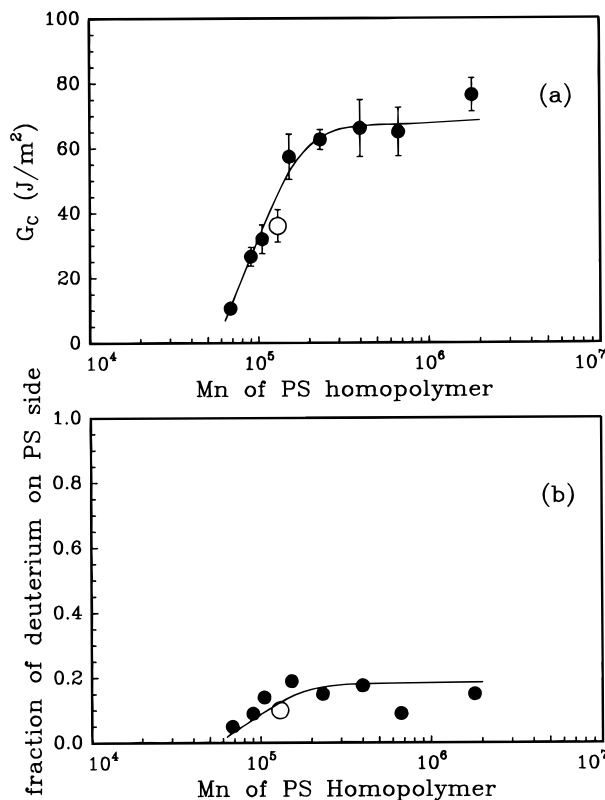


Figure 5. (a) The fracture toughness of the interface is plotted as a function of number average molecular weight of (●) the monodisperse homopolymer PS and (○) the polydisperse PS at $\Sigma = 0.10$ chains/nm² of the 510–540 diblock copolymer. (b) Fraction of the deuterium found on the PS fracture surface, P , plotted versus molecular weight of MPS.

PS for the 800–870 and 510–540 diblock copolymers, respectively. At high \bar{M}_n ($\bar{M}_n \geq 150\,000$), the fraction holds constant at about 0.2. Below $\bar{M}_n \approx 150\,000$, the fraction decreases to nearly zero with decreasing \bar{M}_n of PS for both copolymers. The deuterium fraction data for the polydisperse PS sample seems to fall on the curve that is measured from the monodisperse samples, again indicating that \bar{M}_n is the important molecular weight parameter.

The high G_c values indicate that major plastic deformation occurs during fracture. Optical microscope observations show that the fractured remnants of craze material on the fracture surfaces can be seen for all samples in Figures 4 and 5. Since PS has lower crazing stress than PVP, the craze widens only into the homopolymer PS side of the interface and the craze fibrils finally break down at the crack tip. The plot of deuterium fraction on the PS side, $P (= \Sigma(\text{PS})/\Sigma)$, vs \bar{M}_n shows that the locus of fracture is near the copolymer brush region, where the dPS block of the copolymer and the homopolymer PS meet. There are two main failure mechanisms of the craze fibrils: chain scission and chain disentanglement. Previous experiments by Norton *et al.*¹⁷ with end-functional dPS chains grafted to PS/epoxy interfaces show that the locus of fracture changes from near the PS/epoxy interface, where chain scission of craze fibrils predominately occurs for $N/N_e > 8$, to near the brush tip of the grafting chain where both chain scission and chain disentanglement occur for $N/N_e < 5$, where N is the degree of polymerization of the dPS grafted chain. In our case, N/N_e is equal to 4.6 and 3 for the 800–870 and 510–540 diblock copolymers, respectively. From these observations, our P vs \bar{M}_n ($P \leq 20\%$ for all \bar{M}_n) results indicate that craze fibrils fail

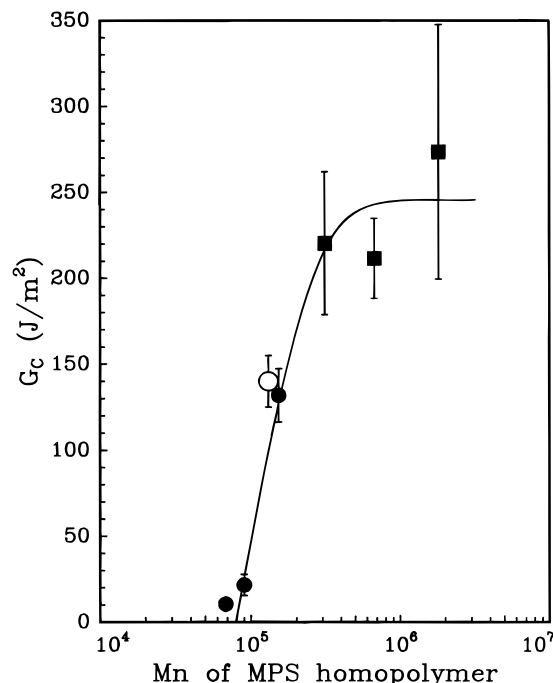


Figure 6. The fracture toughness of the interface is plotted as a function of number average molecular weight of (●) the monodisperse homopolymer PS and (○) the polydisperse PS at $\Sigma = 0.11$ chains/nm² of the 800–870 diblock copolymer. For the filled square data, the fracture occurs between polydisperse PS and monodisperse PS.

by both chain scission and chain disentanglement for $\bar{M}_n \geq 150\,000$ and that the craze fibrils fail predominantly by chain disentanglement for $\bar{M}_n \lesssim 150\,000$.

In Figure 6, the fracture toughness of the PS/PVP interface is plotted as a function of \bar{M}_n of the PS at $\Sigma \approx 0.11$ chains/nm² of the 800–870 diblock copolymer. The characteristic G_c vs \bar{M}_n behavior is also seen in the plot. At higher \bar{M}_n , G_c has a plateau value around 250 J/m², which is larger than the plateau G_c value of 150 J/m² for $\Sigma \approx 0.09$ chains/nm² of the same diblock copolymer. However, for $\bar{M}_n > 200\,000$ the locus of fracture is found to be at the interface between PPS and MPS homopolymers. The fact that the weak interface is now the PPS/MPS one results from incomplete welding at this interface between the PPS and the MPS. But this result also implies that the actual fracture toughness of 800–870 diblock copolymer reinforced interface between MPS and PVP is even larger than 250 J/m² at high \bar{M}_n . As \bar{M}_n decreases from 150 000, the G_c values decrease sharply to ~ 10 J/m². The interface is now found to fail between the polymer brush and the MPS homopolymer. For $G_c < 10$ J/m², it is doubtful that a full craze develops at the interface.

3. Craze Fracture at High Areal Chain Density ($\Sigma \geq \Sigma_{\text{sat}}$). For $\Sigma \geq \Sigma_{\text{sat}} = 0.2$ chains/nm², the diblock copolymer has completely saturated the PS/PVP interface and has started to form a lamellar structure at the interface.⁷ From previous transmission electron microscope (TEM) observations of the PS/PVP interface,⁷ complete coverage by a single lamella occurs at $\Sigma \approx 0.4$ chains/nm² for both copolymers. In Figure 7a, the fracture toughness of the PS/PVP interface is plotted as a function of \bar{M}_n of the PS for $\Sigma \approx 0.55$ chains/nm² of the 510–540 diblock copolymer. The G_c is found to be independent of \bar{M}_n of the MPS and has a constant value of ~ 27 J/m², which is more than twice as large as that for the polydisperse PS, as indicated by the open circle in Figure 7a. In Figure 7b, P has a value ~ 0.40 , which

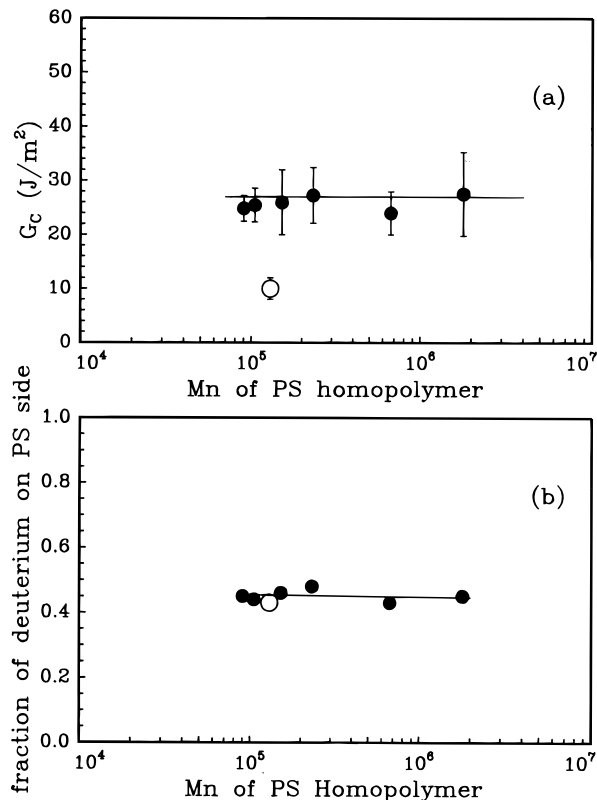


Figure 7. (a) The fracture toughness of the interface is plotted as a function of number average molecular weight of (●) the monodisperse homopolymer PS and (○) the polydisperse PS at $\Sigma = 0.55$ chains/nm² of the 510–540 diblock copolymer. (b) Fraction of the deuterium found on the PS fracture surface, P , plotted versus molecular weight of MPS.

is also independent of \bar{M}_n of the MPS. The results show that for all \bar{M}_n of the MPS, the locus of fracture is near the center of PS lamella nearest to the PVP homopolymer. As was previously reported,⁷ the presence of lamellae greatly decreases the fracture toughness G_c due to two possible reasons. First, the block copolymer lamella has a low fracture toughness since the lamella consists of two polymer brushes repelling each other at their ends. Such brushes have relatively little overlap and thus entanglement. Second, the low molecular weight portion of the homopolymer can also swell the diblock copolymer lamella,^{18,19} resulting in a further decrease in G_c of the lamella. Comparing the G_c values for both MPS and PPS in Figure 7a, it is clear that the fracture toughness G_c is indeed decreased by the low \bar{M}_n fraction of PPS by diluting the already low entanglement between two the polymer brushes.

4. Blending High and Low \bar{M}_n Homopolymers.

In Figure 8a, the fracture toughness of the PS/PVP interface is plotted as a function of volume fraction of low molecular weight MPS ($\bar{M}_n = 4000$) mixed with high molecular weight of MPS ($\bar{M}_n = 670\,000$) at $\Sigma = 0.09$ chains/nm² of the 800–870 diblock copolymers at the interface. It is clear that there is a damaging effect of adding even a relatively small volume fraction, ϕ , of low molecular weight polymer too short to entangle. When this happens, G_c drops from ~ 150 to ~ 10 J/m² at about $\phi \approx 0.3$. In Figure 8b, the value of the fraction of deuterium on PS side, P , decreases monotonically with increasing ϕ of MPS with low \bar{M}_n , indicating that the number of copolymer chains disentangled from the homopolymer PS matrix increases with increasing ϕ of the low \bar{M}_n MPS.

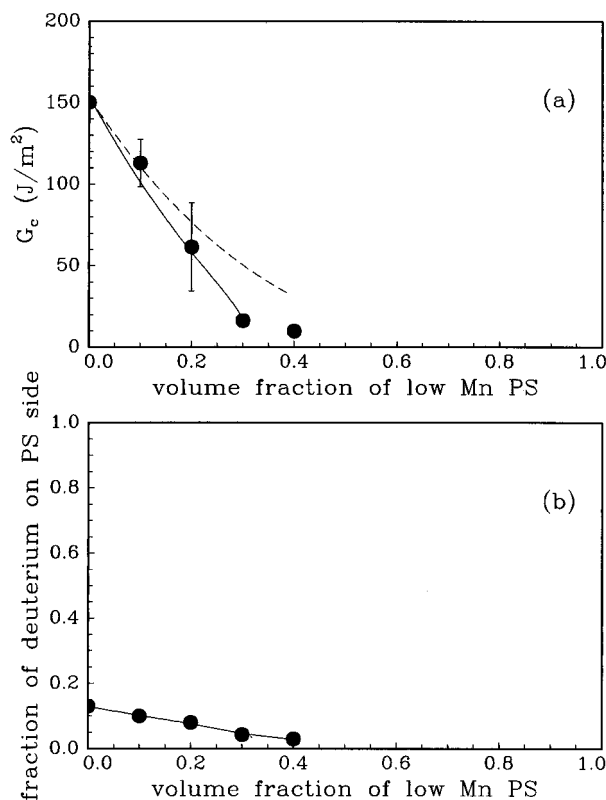


Figure 8. (a) The fracture toughness of the interface is plotted as a function of volume fraction, ϕ , of low \bar{M}_n ($\bar{M}_n = 4000$) of the PS at $\Sigma = 0.09$ chains/nm² of the 800–870 diblock copolymer: (---) asymptotic stress model prediction and (—) full stress field model prediction. (b) Fraction of the deuterium found on the PS fracture surface, P , plotted versus ϕ .

Discussion

The dependence of the interface fracture toughness on the molecular weight of the homopolymer PS enables us to test recent models for the craze breakdown ahead of the crack tip. As mentioned previously, Brown² showed that “cross-tie” fibrils allow the transfer of load from behind the crack tip, thus increasing the stress on the fibrils near the tip of the crack in the craze. The failure criterion is defined as the point at which the stress of the last fibril in a craze, σ_{fibril} , reaches the bond breaking stress of the remaining entangled strands in the fibril, $\Sigma_{\text{eff}} f_b$, where Σ_{eff} is the effective areal density of entangled strands in the fibril and f_b is the force to break a carbon–carbon bond. For a homogeneous polymer, Brown and Hui *et al.*⁹ demonstrate that the fracture toughness is dependent on the underlying craze structure and is given by

$$G_c = 2\pi D(1 - \nu_f)(\Sigma_{\text{eff}} f_b)^2 / (\sigma_c \alpha) \quad (2)$$

where σ_c is the crazing stress, ν_f is the volume fraction of the fibrillated material in the craze, D is the fibril spacing, and α is equal to $\sqrt{(C_{12}/C_{22})}$, where C_{22} and C_{12} are the longitudinal and shear elastic constants of the craze. Taking polymer chain end effects and entanglement density loss effects during crazing into account, Kramer and Berger¹⁰ formulated the effective areal chain density, Σ_{eff} for a homopolymer as follows

$$\Sigma_{\text{eff}} = q\Sigma^\circ (1 - (M_e/q\bar{M}_n)) \quad (3)$$

where q is the probability that an entangled strand in the bulk polymer glass survives the fibrillation during

crazing, Σ° is the areal chain density of entangled strands that cross a plane in the undeformed polymer glass and is given by $\Sigma^\circ = \nu_e d_e/2$, where ν_e and d_e denote, respectively, the strand density and the end-to-end distance of the strand of the entanglement network. The factor $1 - (M_e/q\bar{M}_n)$ is a correction for the chain end segments that cannot form part of the entanglement network but are included in the entanglement density, ν_e .

More recently, Sha *et al.*²⁰ show that for a thin craze, the asymptotic stress field used by Brown and by Hui *et al.* underestimates the stress field at the crack tip fibril. Using a discrete model, Sha *et al.* show that the fracture toughness can be predicted accurately using the continuum model only if the full stress field ahead of crack tip is used. The G_c formula is given by

$$G_c = 2\pi D\sigma_c(1 - \nu_f) \left(-\alpha \ln \left(1 - \left(\frac{\sigma_c}{\Sigma_{\text{eff}} f_b} \right)^2 \right) \right)^{-1} \quad (4)$$

For PS, the parameters that enter eq 4 have been previously estimated ($\sigma_c = 55$ MPa, $\nu_f = 0.25$, $f_b = 2 \times 10^{-9}$ N, $D = 8.65$ nm, $q = 0.6$).^{3,10,24} The only unknown parameter, α , which characterizes the elastic constants of crazed material, can be determined from the G_c measurement as a function of molecular weight of a pure homopolymer PS using both eqs 3 and 4. The value of α ($\alpha = 0.026$) thus determined corresponds to a maximum fracture toughness of ~ 1000 J/m² for a high molecular weight PS, which is consistent with the literature G_c value for PS.²²

We can rewrite eq 4 to express Σ_{eff} explicitly, i.e.,

$$\Sigma_{\text{eff}} = \frac{\sigma_c}{f_b \sqrt{1 - \exp(-G_c^*/G_c)}} \quad (5)$$

where $G_c^* = 2\pi(1 - \nu_f)\sigma_c D/\alpha$. Equation 5 can then be used to estimate the areal density of entanglement, Σ_{eff} , between the block copolymer and the homopolymer PS if the G_c of the interface is measured. The parameters that are obtained for the pure homopolymer PS can also be used in the PS/PVP interface case since the craze only widens into the PS side. The craze structure near the PS/PVP interface is assumed to be unchanged from that of a craze in the pure homopolymer PS. In parts a and b of Figure 9, Σ_{eff} is plotted as a function of \bar{M}_n of MPS for $\Sigma = 0.09$ chains/nm² of the 800–870 diblock copolymer and for $\Sigma = 0.10$ chains/nm² of the 510–540 diblock copolymer, respectively. The dashed line, $\Sigma_{\text{eff}}^{\text{MPS}}$, represents the areal chain density of the pure homopolymer MPS as a function of \bar{M}_n of the MPS obtained by using eq 3. The measured areal density of the block copolymer, $\Sigma_{\text{eff}}^{\text{FRES}}$, represented by a solid line, is given by $q\Sigma$ where Σ is the areal chain density of the block copolymer as measured using FRES. $\Sigma_{\text{eff}}^{\text{FRES}}$ as formulated is the maximum areal chain density of the block copolymer after crazing since the formula does not consider chain end effect on the block copolymer. Furthermore, since $\Sigma_{\text{eff}}^{\text{MPS}}$ is always larger than $\Sigma_{\text{eff}}^{\text{FRES}}$ for $\bar{M}_n \geq 70\,000$ in Figure 9a,b, $\Sigma_{\text{eff}}^{\text{FRES}}$ is also the limiting areal density of the entanglement between the block copolymer and the homopolymer PS. The solid circles represent the effective areal density, $\Sigma_{\text{eff}}^{\text{calc}}$, that is obtained using eq 5 from the measurement of G_c vs \bar{M}_n of the MPS. For the 800–870 diblock copolymer as shown in Figure 9a, $\Sigma_{\text{eff}}^{\text{calc}}$ has a value close to $\Sigma_{\text{eff}}^{\text{FRES}}$ for $\bar{M}_n \approx 150\,000$. However, for $70\,000 \lesssim \bar{M}_n \lesssim 150\,000$,

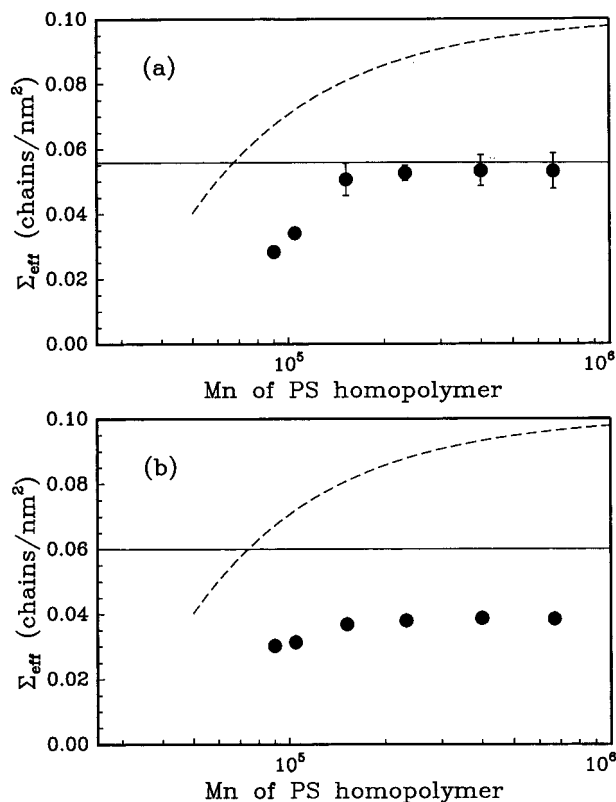


Figure 9. Areal chain densities of the block copolymer and the homopolymer PS are plotted as a function of \bar{M}_n of the MPS. $\Sigma_{\text{eff}}^{\text{MPS}}$, represented by the dashed-dotted line, is the areal chain density of the homopolymer MPS using eq 3. $\Sigma_{\text{eff}}^{\text{FRES}}$, represented by a solid line, is given by $q\Sigma$ where Σ is the areal chain density of the block copolymer as measured using FRES. The dashed lines represent the effective areal density, $\Sigma_{\text{eff}}^{\text{calc}}$, that is obtained using eq 5 from the measurement of G_c vs \bar{M}_n of the MPS. (a) The interface reinforced with the 800–870 diblock copolymer at $\Sigma = 0.09$ chains/nm². (b) The interface reinforced with the 510–540 diblock copolymer at $\Sigma = 0.10$ chains/nm².

$\Sigma_{\text{eff}}^{\text{calc}}$ is smaller than $\Sigma_{\text{eff}}^{\text{FRES}}$ and $\Sigma_{\text{eff}}^{\text{calc}}$ decreases with decreasing \bar{M}_n . As shown previously, for the 800–870 diblock copolymer reinforced interface, the craze fails by both chain scission and chain disentanglement mechanisms. It should be noted that $\Sigma_{\text{eff}}^{\text{calc}}$ is the areal chain density computed assuming that the craze fails by the chain scission mechanism only. For $70\,000 \leq \bar{M}_n \leq 150\,000$, the apparent areal density, $\Sigma_{\text{eff}}^{\text{FRES}}$, is larger than the actual areal chain density, $\Sigma_{\text{eff}}^{\text{calc}}$, for supporting crazing since craze fails predominately by chain disentanglement of the 800–870 block copolymer from the PS. For $\bar{M}_n \geq 150\,000$, chain scission is the active mechanism for craze failure. While some chain disentanglement mechanism may also occur in this molecular weight regime, it seems to play a minor role in final craze failure. A different situation is shown in Figure 9b. For the interface reinforced with the 510–540 diblock copolymer, $\Sigma_{\text{eff}}^{\text{calc}}$ is smaller than $\Sigma_{\text{eff}}^{\text{FRES}}$ for all \bar{M}_n of the MPS. Since the molecular weight of dPS of the 510–540 diblock copolymer is smaller than that for the 800–870 diblock copolymer, chain disentanglement of the 510–540 diblock copolymer from the PS entangled network of a craze is even more likely for all \bar{M}_n of the MPS. Indeed, for $\bar{M}_n \geq 200\,000$, both the chain disentanglement and chain scission mechanism are active. For $70\,000 \leq \bar{M}_n \leq 200\,000$, the craze fails predominately by chain disentanglement.

In the experiment where the interface was glazed with a blend of PS with high and low \bar{M}_n , the areal chain density, Σ_{eff} , of diluted entanglement network can be calculated as follows:²⁰

$$\nu_e = [\nu_e]\phi^2 \quad (6)$$

$$d_e = [d_e]/\phi^{1/2} \quad (7)$$

$$M_e = [M_e]/\phi \quad (8)$$

where brackets denotes the value for the undiluted high molecular weight species and ϕ is the volume fraction of the low molecular weight component in the blend. Based on eq 3, Σ_{eff} is then given by

$$\Sigma_{\text{eff}} = q\Sigma\phi^{3/2}(1 - M_e/q\phi\bar{M}_n) \quad (9)$$

By combining eq 9 with eq 2 or 4, we can obtain the relationship of G_c vs ϕ for $\Sigma = 0.09$ chain/nm² of the 800–870 diblock copolymer at the interface between PVP and a mixture of $\bar{M}_n = 4000$ and $\bar{M}_n = 670\,000$ PS. In Figure 8a, the prediction from the asymptotic stress field model (eq 2) is plotted as the dashed line and the prediction from the full stress field model (eq 4) is plotted as the solid line. The full stress field model fits the experimental data well for all ϕ . The asymptotic stress field model, on the other hand, overestimates the fracture toughness for $\phi = 0.25$ – 0.4 , where a narrow and weak craze forms at the interface.

The central parameter that determines the fracture toughness of the polymer interface is the effective areal density of entangled strand, Σ_{eff} , between the diblock copolymers and the homopolymers. Using self-consistent mean field (SCMF) calculation,²⁵ an estimate of the entanglement structure at the molecular level between block copolymer and homopolymer can be obtained. However, at present the available micromechanics models do not accurately describe the failure of a craze at the interface in the regime where chain disentanglement dominates. The models do not describe the regime where both chain scission and disentanglement are important. The experimental results presented here nevertheless can serve to test future theoretical models for craze growth by chain disentanglement or a combination of chain disentanglement and scission.

Conclusions

We have investigated the molecular weight dependence of the homopolymer on G_c for $4M_e < \bar{M}_n < 10M_e$ at various values of Σ of the diblock copolymers at the interface. The results can be summarized as follows.

(1) \bar{M}_n (not \bar{M}_w) is the controlling moment of the homopolymer molecular weight distribution for interface fracture.

(2) In the chain scission regime, the fracture toughness is low and is independent of the \bar{M}_n of the homopolymer PS. The diblock copolymer is broken near its joint as the interface fails.

(3) In the crazing regime with the condition of $\Sigma \leq \Sigma_{\text{sat}}$, the fracture toughness strongly depends on the \bar{M}_n of the homopolymer PS. The fracture toughness increases sharply with increasing \bar{M}_n in the regime of $70\,000 \leq \bar{M}_n \leq 150\,000$ and then levels off for higher \bar{M}_n . Chain disentanglement of the block copolymer from the craze prevails for $\bar{M}_n \leq 150\,000$. A chain scission mechanism prevails for $\bar{M}_n \geq 150\,000$ for the 800–870 diblock copolymer reinforced interface. However, both

chain scission and chain disentanglement mechanisms are active for $\bar{M}_n \geq 70\,000$ for the 510–540 diblock copolymer reinforced interface. The polydisperse PS/PVP interface has a fracture toughness consistent with its \bar{M}_n .

(4) In the crazing regime for the condition $\Sigma \geq \Sigma_{\text{sat}}$, fracture occurs in the center of PS lamellae for both PPS and MPS samples. However, the polydisperse sample has a fracture toughness lower than the monodisperse sample of the same \bar{M}_n . The low molecular weight portion of the PPS appears to swell the lamellar structure and decreases the fracture toughness.

(5) Adding a small volume fraction of homopolymer PS chains that are too short to entangle decreases the fracture toughness of the interface significantly.

Acknowledgment. We gratefully acknowledge the support from the Material Science Center (MSC) at Cornell University, which is funded by the National Science Foundation. C.-A.D. thanks the Cornell-Industry Electronic Packaging Alliance Program for its partial support. J.W. is supported by a grant from Showa Denko, K. K., Japan. We also benefited from the use of the ion beam analysis facility of the MSC at Cornell University.

References and Notes

- (1) Fayt, R.; Jérôme, R.; Teyssié, Ph. *J. Polym. Sci., Polym. Phys. Ed.* **1989**, *27*, 775.
- (2) Brown, H. R. *Macromolecules* **1991**, *24*, 2752.
- (3) Creton, C.; Kramer, E. J.; Hui, C.-Y.; Brown, H. R. *Macromolecules* **1992**, *25*, 3075.
- (4) Brown, H. R.; Char, K.; Deline, V. R.; Green, P. F. *Macromolecules* **1993**, *26*, 4155.
- (5) Char, K.; Brown, H. R.; Deline, V. R. *Macromolecules* **1993**, *26*, 4164.
- (6) Washiyama, J.; Kramer, E. J.; Hui, C.-Y. *Macromolecules* **1993**, *26*, 2928.
- (7) Washiyama, J.; Creton, C.; Kramer, E. J.; Xiao, F.; Hui, C.-Y. *Macromolecules* **1993**, *26*, 6011.
- (8) Creton, C.; Brown, H. R.; Deline, V. R. *Macromolecules* **1994**, *27*, 1774.
- (9) Hui, C.-Y.; Ruina, A.; Creton, C.; Kramer, E. J. *Macromolecules* **1992**, *25*, 3948.
- (10) Kramer, E. J.; Berger, L. L. *Adv. Polym. Sci.* **1990**, *91/92*, 1.
- (11) de Gennes, P.-G. *Europhys. Lett.* **1991**, *15*, 191.
- (12) Shull, K. R.; Kramer, E. J.; Hadziioannou, G.; Tang, W. *Macromolecules* **1990**, *23*, 4780.
- (13) Mills, P. J.; Green, P. F.; Palmström, C. J.; Mayer, J. W.; Kramer, E. J. *J. Appl. Phys. Lett.* **1984**, *45*, 957.
- (14) Washiyama, J.; Creton, C.; Kramer, E. J. *Macromolecules* **1992**, *25*, 4751.
- (15) Kanninen, M. F. *Int. J. Fracture* **1973**, *9*, 83.
- (16) Xiao, F.; Hui, C.-Y.; Washiyama, J.; Kramer, E. J. *Macromolecules* **1994**, *27*, 4382.
- (17) Norton, L. J.; Smigolova, V.; Pralle, M. U.; Hubenko, A.; Dai, K. H.; Kramer, E. J.; Hahn, S.; Berglund, C.; Dekoven, B. *Macromolecules* **1995**, *28*, 1999.
- (18) Hashimoto, T.; Shibayama, M.; Kawai, H. *Macromolecules* **1980**, *13*, 1237.
- (19) Winey, K. I.; Thomas, E. L.; Fetters, L. J. *Macromolecules* **1991**, *24*, 6182.
- (20) Sha, Y.; Hui, C.-Y.; Ruina, A.; Kramer, E. J. *Macromolecules* **1995**, *28*, 2450.
- (21) Hui, C.-Y.; Kramer, E. J. *Polym. Eng. Sci.* **1995**, *35*, 419.
- (22) Wool, R. P.; Yuan, B.-L.; McGarel, O. J. *Polym. Eng. Sci.* **1989**, *29*, 1340.
- (23) Equations 2 and 4 are based on the model of a crack propagating in the center of the craze. In our case, the craze widens only into one side (PS side) of the interface. Thus, the G_c for interface failure in our case is only half of that predicted from eqs 2 and 4.
- (24) Berger, L. L. *Macromolecules* **1989**, *22*, 3162.
- (25) Shull, K. R.; Kramer, E. J. *Macromolecules* **1990**, *23*, 4769.

MA960533L